Journal of Radiation Research, Vol. 63, No. 2, 2022, pp. 192–201
https://doi.org/10.1093/jrr/rrab125
Advance Access Publication: 21 January 2022

Irradiated microvascular endothelial cells may induce bystander effects in neural stem cells leading to neurogenesis inhibition

Linlin Ma[1], Zhujing Ye[1], Yarui Zhang[1], Wenyu Shi[2], Jingdong Wang[1] and Hongying Yang[1,*]

[1]State Key Laboratory of Radiation Medicine and Protection, School of Radiation Medicine and Protection, Medical College of Soochow University/Collaborative Innovation Center of Radiation Medicine of Jiangsu Higher Education Institutions, 199 Renai Road, Suzhou Industrial Park, Suzhou, Jiangsu Province, P. R. China 215123
[2]Department of Radiotherapy and Oncology, Second Affiliated Hospital of Soochow University, 1055 Sanxiang Road, Suzhou, Jiangsu Province, 215004, P. R. China
*Corresponding author. H. Yang, Tel: +86-512-65882637; Fax: +86-512-65884830; Email: yanghongying@suda.edu.cn
(Received 13 September 2021; revised 18 November 2021; editorial decision 9 December 2021)

ABSTRACT

Radiation-induced neurocognitive dysfunction (RIND) has attracted a lot of attention lately due to the significant improvement of the survival of cancer patients after receiving cranial radiotherapy. The detailed mechanisms are not completely understood, but extensive evidence supports an involvement of the inhibition of hippocampal neurogenesis, which may result from radiation-induced depletion of neural stem cells (NSCs) as well as the damage to neurogenic niches. As an important component of neurogenic niches, vascular cells interact with NSCs through different signaling mechanisms, which is similar to the characteristics of radiation-induced bystander effect (RIBE). But whether RIBE is involved in neurogenesis inhibition contributed by the damaged vascular cells is unknown. Thus, the purpose of the present study was to investigate the occurrence of RIBEs in non-irradiated bystander NSCs induced by irradiated bEnd.3 vascular endothelial cells in a co-culture system. The results show that compared with the NSCs cultured alone, the properties of NSCs were significantly affected after co-culture with bEnd.3 cells, and further change was induced without obvious oxidative stress and apoptosis when bEnd.3 cells were irradiated, manifesting as a reduction in the proliferation, neurosphere-forming capability and differentiation potential of NSCs. All these results suggest that the damaged vascular endothelial cells may contribute to neurogenesis inhibition via inducing RIBEs in NSCs, thus leading to RIND.

Keywords: radiation-induced neurocognitive dysfunction (RIND); radiation-induced bystander effect (RIBE); bEnd.3 cells; neural stem cells (NSCs); neurogenesis

INTRODUCTION

While advanced radiation therapy (RT) technology significantly increases the overall survival of patients with primary and metastatic brain tumors, it may cause injury to the brain. Among different types of radiation-induced brain injury, neurocognitive dysfunction may occur at a ratio as high as 50–90% in patients who undergo whole brain radiation therapy (WBRT) and survive for more than six months [1]. The symptoms of radiation-induced neurocognitive dysfunction (RIND) include intellectual impairment, memory loss and dementia, which progress over time, thus severely deteriorating the quality of life of cancer patients after RT. Although the mechanisms underlying RIND are still unclear, a lot of evidence indicates that radiation-caused injury to the hippocampus, a crucial area of the brain in charge of learning and memory, is responsible for the occurrence of RIND [2]. It has been found that the neurocognitive functions of children receiving cranial RT were negatively correlated to the radiation dose to the hippocampus [3], and cognitive functions may be preserved via hippocampus avoidance during WBRT [4, 5]. More specifically, radiation-induced hippocampal neurogenesis inhibition plays an important role. Pharmacologic agents such as Baicalein and lithium can ameliorate RIND through attenuating radiation-induced neurogenesis inhibition [6, 7]. Moreover, neural stem cell (NSC) transplantation

can restore cognitive function, in which a certain percentage of engrafted NSCs survive, migrate, differentiate and integrate into the hippocampus [8].

Radiation-induced damage to NSCs is one of the major factors for radiation-induced neurogenesis inhibition. In addition to direct damage to NSCs, the non-targeted damage to NSCs, e.g. radiation-induced bystander effects (RIBEs) may also kill NSCs, inhibit NSC proliferation and differentiation, eventually leading to neurogenesis inhibition [9]. RIBEs, referring to the biological changes observed in non-irradiated cells when they receive intercellular communication signaling from nearby irradiated cells [10]. In spite of the intensive study on RIBEs in the past 30 years, it still remains unclear what role RIBEs play in radiation-induced tissue injury. We have previously demonstrated that irradiated cancer cells can induce bystander effects in NSCs in turn contribute to neurogenesis inhibition and cognitive impairment, suggesting that RIBEs may be one of the mechanisms underlying RIND [11].

Neurogenic niches comprising NSCs and other cell types such as endothelial cells, microglia, etc. provide a suitable microenvironment for neurogenesis [12, 13]. Therefore, the long-lasting perturbations in neurogenic niches caused by radiation, e.g. inflammatory response and abnormal association between NSCs/precursor cells and microvasculature also contribute to radiation-induced neurogenesis inhibition by inhibiting the proliferation and neuronal differentiation of NSCs [14]. Besides these long-term alterations, radiation causes endothelial cell damage and vascular disruption soon after exposure [15]. And damage from directly irradiated endothelial cells can be transferred to surrounding non-irradiated endothelial cells through bystander signaling leading to more extensive damage [16]. But it is not clear whether the damaged endothelial cells can induce RIBEs in NSCs, thus causing NSC dysfunction.

Therefore, this study aimed to evaluate how irradiated microvascular endothelial cells affected non-irradiated NSCs. It was found that in a co-culture system irradiated bEnd.3 endothelial cells induced medium-mediated bystander effects in non-irradiated NSCs, which manifested as reduced cell proliferation, impaired self-renewal and differentiation.

MATERIALS AND METHODS

Cell culture

bEnd.3 cells purchased from Procell Life Science & Technology Co. Ltd (China) were cultured in DMEM medium (Gibco, USA) containing FBS (10%, Gibco, USA) and Penicillin-Streptomycin (1%, Beyotime, China) in an incubator with 5% CO_2 at 37°C. The doubling time of bEnd.3 cells growing exponentially (passages 12–20) used for the experiments was approximately 20–24 h, which was calculated by the formula: Doubling time = duration × ln (2)/ln (final cell numbers/initial cell number).

The Medical Experimental Animal Care Guidelines of Soochow University were strictly complied with in all animal procedures. As previously described [17], NSCs were isolated from cerebral cortex of the fetuses growing in C57BL/6 mice at E12.5 days of gestation.

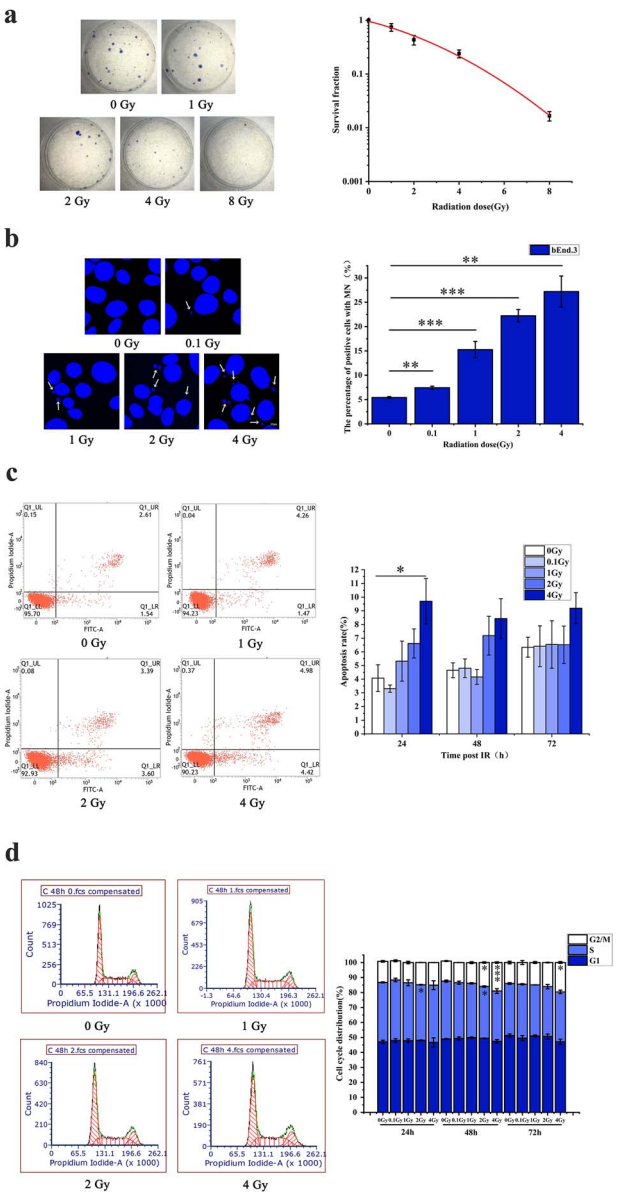

Fig. 1. bEnd.3 cells are radiosensitive. (a) Representative photos of bEnd.3 clones and the survival curve of bEnd.3 cells after X-ray exposure. (b) Representative images of MN and the MN formation frequency of bEnd.3 cells 48 h after X-irradiation. (c) Representative flow cytometry dot plots for apoptosis at 24 h post IR and quantification of apoptosis rate of bEnd.3 cells after X-irradiation with different doses. (d) Representative cell cycle histograms for bEnd.3 cells at 48 h post X-irradiation and quantification of cell cycle distribution of bEnd.3 cells at different times after different X-irradiation doses. $p < 0.05$, 0.01 and 0.001 between two groups are denoted by *, ** and *, respectively.**

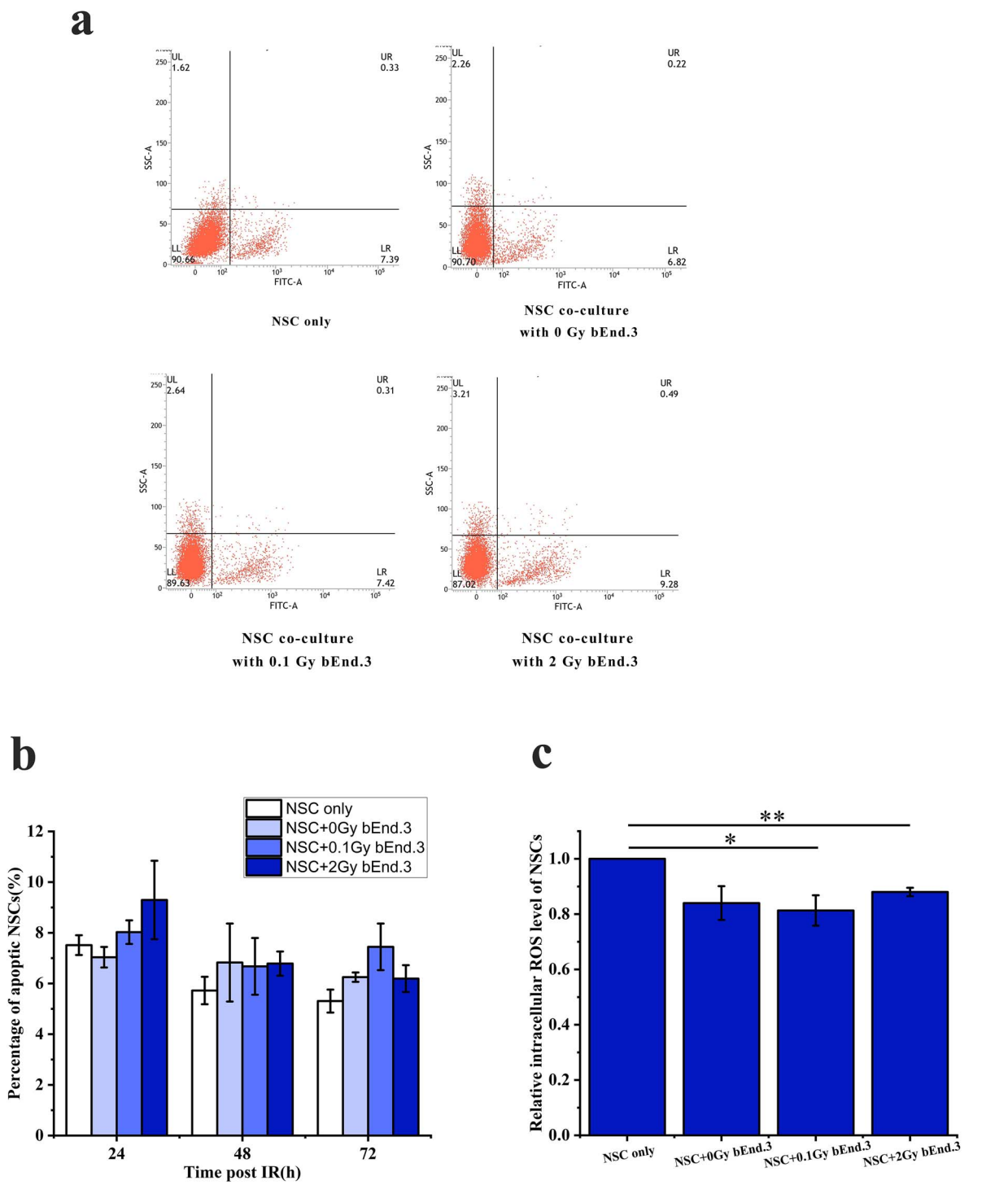

Fig. 2. Irradiated bEnd.3 cells did not induce significant apoptosis and oxidative stress in bystander NSCs. (a) Representative flow cytometry dot plots for apoptotic NSCs after 24 h of co-culture with bEnd.3 cells. (b) Apoptosis rate of NSCs after co-culture with bEnd.3 cells. (c) Intracellular ROS levels of NSCs after co-culture with bEnd.3 cells for 1 h. $p < 0.05$ and 0.01 between two groups were denoted by * and **, respectively.

The obtained NSCs were then cultured in an incubator with 5% CO_2 at 37°C in the proliferation medium, i.e. DMEM-F12 (Gibco, USA) supplemented with B27 (2%, Gibco, USA), bFGF (20 ng/ml, Sigma-Aldrich, USA), EGF (20 ng/ml, Sigma-Aldrich, USA) and Penicillin-Streptomycin (1%, Beyotime) in T25 culture flasks at a starting density of 2×10^5 cells/ml. NSCs were sub-cultured every 4 days after neurospheres were formed. The NSCs used in the experiments were from passage 3 to passage 6 with a doubling time of 24 h.

Irradiation and co-culture system

7×10^4–1×10^5 bEnd.3 cells per well were plated on the coverslips in 12-well plates. After 24 h, bEnd.3 cells were irradiated by RAD SOURCE RS2000 X-ray machine (160 kVp, 25 mA, 0.3-mm Cu filter, USA) at room temperature (RT) at 1.16 Gy/min, which was determined by Accu-Dose™ Radiation Measurement System (Radcal Corporation, USA). bEnd.3 cells receiving 0 Gy of X-rays, i.e. sham-irradiated cells were used as control. Meanwhile, 2×10^5 NSCs were seeded in each well of 6-well plates. Immediately after irradiation, the coverslips with bEnd.3 cells were transferred to transwell culture inserts with a membrane of 0.4 μm pore size (Millipore, USA), and the inserts were then put into co-culture with NSCs in 6-well plates. Thus the irradiated bEnd.3 cells and unirradiated NSCs shared the same NSC medium but were not in direct contact.

Clonogenic assay

Depending on the radiation dose, bEnd.3 cells were plated into 60-mm petri dishes with different cell numbers. After replenished with fresh medium 24 h later, cells were X-irradiated. The cells were kept in culture at 37°C for two weeks. After fixed with methanol followed by methylene blue staining (Sangon Biotech) at RT for 15 min for each step, the colonies containing at least 50 cells were counted. The surviving fraction (SF) of irradiated cells was calculated using the formula: SF = number of colonies counted/(number of cells plated × (PE/100)). PE represents plating efficiency of sham-irradiated bEnd.3, which was determined as 34%. The cell survival dose–response curve of bEnd.3 cells was plotted using the survival fraction against the irradiation dose.

Micronucleus (MN) formation assay

bEnd.3 cells plated on coverslips were irradiated with X-rays. After 48 h, the cells were fixed with methanol/acetic acid fixative (V:V = 3:1) for 10 min at RT and let air dry. Following rehydration, the cells were stained with 5 mg/ml 4′, 6′-diamidimo-2-phenylindole (DAPI, Beyotime, China) for 5 min. The nuclei with micronucleus were counted under a fluorescence microscope (Leica DM2000). At least 1000 cells per sample were examined. Micronucleus frequency was calculated by the formula: The percentage of positive cells with micronucleus = (the number of positive cells with micronucleus/the number of cells counted) × 100%.

Apoptosis determined by flow cytometry

bEnd.3 cells were X-irradiated 24 h after plating. The cells were collected at different times after irradiation. For NSCs, after co-culture with bEnd.3 cells for different times, NSCs were dispersed into single cells and collected. The collected cells were then resuspended in Annexin V-FITC binding solution and stained with Annexin V FITC/PI (BD Biosciences, USA) for 15 min at RT. Apoptotic cells were determined on a flow cytometer (BD FACSVerse, USA). ModFit LT3.2 Software was used for quantification of apoptosis.

Cell cycle distribution determined by flow cytometry

bEnd.3 cells were X-irradiated. At 24, 48 and 72 h post IR, cells were harvested and fixed in 70% ethanol overnight at 4°C. The cells were washed with cold PBS and stained with propidium iodide (PI) (0.1 mg/ml) in the dark. Cell cycle distribution was then determined on a flow cytometer (BD FACSVerse, USA). ModFit LT3.2 Software was used to analyze the data.

Measurement of intracellular reactive oxygen species (ROS)

The intracellular ROS levels of NSCs were determined with Cellular ROS Detection Assay Kit (Abcam, UK). NSCs were incubated with 20 μM DCFDA at 37°C for 30 min in the dark followed by co-culture with bEnd.3 cells. One hour later, NSCs were collected and suspended in 1.5 ml Eppendorf tubes with DMEM/F12 free of phenol red and B27, then the ROS level of NSCs was measured on a BD FACSVerse flow cytometer. BD FACSuite Software was used to analyze the data.

Cell proliferation assay

The neurospheres formed by NSCs co-cultured with bEnd.3 cells for 72 h were harvested and dispersed into single cells. Scepter Automated Cell Counter (Millipore, USA) was used to count NSC number.

Measurement of neurosphere size

Single cell suspension was made out of the neurospheres formed by NSCs co-cultured with bEnd.3 cells for 72 h. The NSCs were then seeded into a 96-well plate and cultured at 37°C for 72 h. Photos of the neurospheres of each group were taken using a light microscope (Olympus, IX73, Japan). Diameter of the neurospheres was measured using Image J.

Stemness maintenance of NSCs assessed by immunofluorescent microscopy

Immunofluorescence staining of nestin was performed to evaluate the stemness maintenance of NSCs [18]. The NSCs co-cultured with bEnd.3 cells for 72 h were re-seeded in 12-well plates containing poly-D-lysine-coated coverslips and cultured in the proliferation medium at 37°C. Two hours later, the cells were fixed in 4% paraformaldehyde for 15 min at RT. Following permeabilization and blocking, the NSCs were sequentially incubated with anti-nestin antibody (Genetex, USA) at 4°C overnight and cy3-conjugated goat anti-rabbit secondary antibody (Beyotime, China) for 1 h at RT. The cells were examined under a fluorescence microscope (FV1200, Olympus, Japan) after counter-stained with DAPI (5 μg/ml, Beyotime, China) for 5 min. At least 500 cells per sample were examined.

Differentiation potential of NSCs evaluated by immunofluorescent microscopy

The NSCs co-cultured with bEnd.3 cells for 72 h were re-seeded on poly-D-lysine-coated coverslips in 12-well plates and cultured at 37°C for 72 h in neuronal differentiation medium (DMEM/F12 containing penicillin-streptomycin (1%), B27 (2%), retinoic acid (5 mM) and FBS (0.5%)) and glial differentiation medium (DMEM/F12 containing penicillin-streptomycin (1%), B27 (2%), forskolin (5 mM) and FBS (1%)), respectively. As described [11, 17], the cells were fixed and immunostained for Tuj1 and GFAP, respectively. The stained cells were photographed using a FV1200 fluorescence microscope. For analysis of

positive cells, at least 500 cells per sample were examined. For analysis of neurites and protrusions, 50 neuronal/glial cells were measured for each sample.

Statistical analysis

The data are presented as the means of three independent experiments ± standard error (SEM). Difference between any two groups was analyzed using one-way ANOVA followed by Tukey's multiple comparison test with Origin Pro 2019b software. The difference between groups was considered statistically significant when $p < 0.05$.

RESULTS

bEnd.3 cells were radiosensitive

To better understand how irradiated bEnd.3 endothelial cells affected unexposed NSCs, we first assessed the radiosensitivity of bEnd.3 cells. As shown in Fig. 1a, after exposed to X-irradiation, the colony formation of bEnd.3 cells significantly decreased in a dose-dependent manner. Furthermore, the frequency of MN formation of bEnd.3 cells increased along with the increase of dose. The percentage of positive cells with MN increased by 37% even after exposed to 0.1 Gy (Fig. 1b). Moreover, 24 h after exposed to X-rays, we detected obvious apoptosis of bEnd.3, particularly with 2 and 4 Gy. And this trend of the increase in apoptosis rate last for at least another 24 h (Fig. 1c). Additionally, 48 h after 2 and 4 Gy of X-irradiation, bEnd.3 cells showed obvious G2/M arrest, and this trend persisted until 72 h after irradiation (Fig. 1d). All these data indicated that bEnd.3 cells were sensitive to IR. Thus, two doses, i.e. 0.1 and 2 Gy were chosen for the following RIBE experiments.

Irradiated bEnd.3 cells did not cause significant apoptosis and oxidative stress in non-irradiated NSCs

Neurogenesis relies heavily on the status of NSCs. To explore whether damaged endothelial cells by IR would inhibit neurogenesis through RIBEs, we first investigated whether irradiated bEnd.3 cells induced apoptosis in unirradiated NSCs. As shown in Fig. 2a and 2b, there was a slight increase in the apoptosis rate of NSCs after 24 h of co-culture with irradiated bEnd.3 cells when compared with sham control, i.e. the NSCs co-cultured with sham-irradiated bEnd.3 cells, but the difference was not statistically significant. And this trend disappeared after 48 and 72 h of co-culture. These data suggested that irradiated bEnd.3 cells did not induce significant apoptosis of unexposed NSCs through a medium-mediated mechanism.

It is common that irradiated cells quickly induce oxidative stress in unexposed bystander cells [19, 20]. Interestingly, compared with the NSCs cultured alone, the intracellular ROS levels of NSCs decreased after co-culture with sham-irradiated bEnd.3 cells for 1 h, and they did not increase obviously when bEnd.3 cells were irradiated (Fig. 2c), indicating that bystander oxidative stress did not occur in non-irradiated NSCs when co-culture with irradiated bEnd.3 cells.

Irradiated bEnd.3 cells reduced the proliferation and self-renewal ability of non-irradiated NSCs

We previously observed a reduction in the proliferation and self-renewal ability of NSCs after co-culture with irradiated tumor cells [11], indicating that irradiated tumor cells could inhibit the proliferation and stemness of non-irradiated NSCs through medium-mediated bystander signaling. Here we examined whether irradiated bEnd.3 endothelial cells affected the cell proliferation and self-renewal ability of non-irradiated NSCs. We found that, compared with the NSCs cultured alone, the proliferation of NSCs co-cultured with bEnd.3 cells decreased significantly. Specifically, after co-culture with sham-irradiated, 0.1 and 2 Gy-irradiated bEnd.3 cells, the NSC number decreased by 47%, 54% and 69%, respectively (Fig. 3a), although the difference between sham-irradiated and irradiated groups was not statistically significant. These results suggested that co-culture with bEnd.3 cells inhibited the proliferation of NSCs and irradiated bEnd.3 cells may cause further inhibition.

Furthermore, we assessed neurosphere formation of NSCs co-cultured with bEnd.3 cells by measuring neurosphere diameter. Compared with the NSCs cultured alone, the mean diameter of the neurospheres formed by NSCs co-cultured with sham-irradiated, 0.1 and 2 Gy-irradiated bEnd.3 cells decreased by 5%, 14% and 17%, respectively (Fig. 3b). These results indicated that the neurosphere-forming ability of NSCs was slightly inhibited by co-culture with bEnd.3 cells and further inhibition was induced by irradiated bEnd.3 cells.

In addition, we evaluated the stemness of bystander NSCs by detecting the expression of nestin, a widely used marker for NSCs [21]. Compared with the NSCs cultured alone, the percentage of nestin-positive NSCs decreased by 26%, 30% and 37% after co-culture with sham-irradiated, 0.1 and 2 Gy-irradiated bEnd.3 cells, respectively (Fig. 3c). These results suggested that the stemness maintenance ability of NSCs reduced after co-culture with bEnd.3 cells, and this reduction was more significant when bEnd.3 cells were irradiated.

Irradiated bEnd.3 cells inhibited the differentiation ability of bystander NSCs

After 72 h of co-culture with bEnd.3, we found that the differentiation ability of NSCs was inhibited. When culture in neuronal differentiation medium, compared with the NSCs cultured alone, the percentage of Tuj1-positive cells decreased by 42% after co-culture with sham-irradiated bEnd.3 cells; after co-culture with bEnd.3 cells X-irradiated with 0.1 and 2 Gy, this percentage decreased by 68% and 79%, respectively (Fig. 4a and 4b). Moreover, the total number of neurites and the mean length of the longest neurites of 50 Tuj1-positive cells in each group were examined. The results show that the neuronal cells differentiated from the NSCs cultured alone had (116 ± 11) neurites with an average length of (40.38 ± 1.06) μm for the longest neurites, while the neuronal cells differentiated from the NSCs cultured with sham-irradiated bEnd.3 cells had (81 ± 1) neurites with an average length of (30.50 ± 2.53) μm for the longest neurites. For the group of NSCs co-cultured with 0.1 Gy-irradiated bEnd.3 cells, the neuronal cells had (48 ± 6) neurites with an average length of (24.90 ± 1.41) μm for the longest neurites. For the group of NSCs co-cultured with 2 Gy-irradiated bEnd.3 cells, the neuronal cells had (42 ± 1) neurites with an average length of (18.34 ± 0.82) μm for the longest neurites (Fig. 4c and 4d). These data suggested that co-culture with bEnd.3 cells reduced the

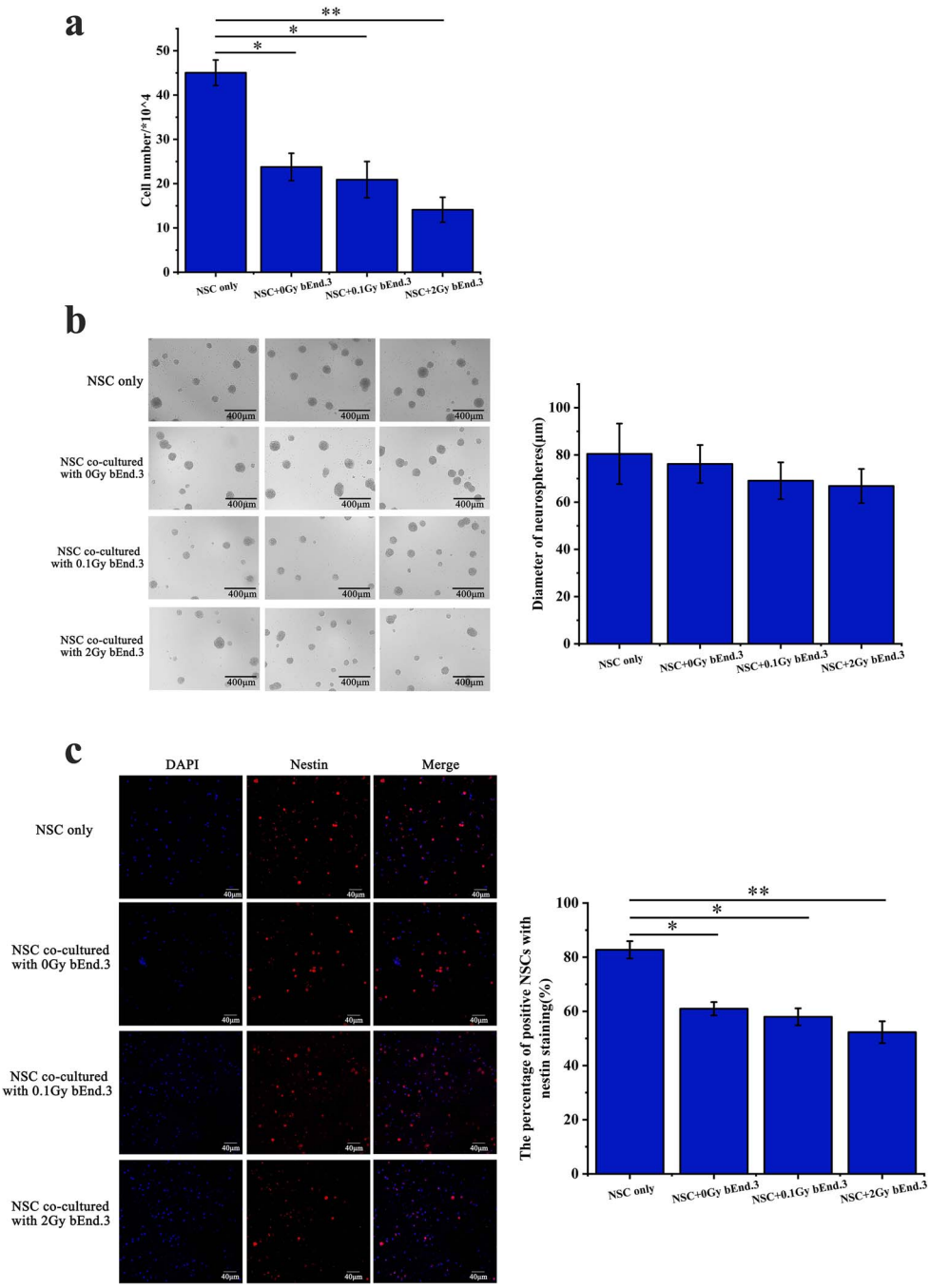

Fig. 3. The proliferation and self-renewal ability of bystander NSCs were inhibited. (a) The NSC number after co-culture with bEnd.3 cells for 72 h. (b) Photos of neurospheres formed by bystander NSCs and quantification analysis of the diameters of neurospheres. (c) Fluorescence images of nestin expression of bystander NSCs and the percentage of nestin-positive NSCs. Blue and red fluorescence indicate DAPI and nestin staining, respectively. $p < 0.05$ and 0.01 between two groups were denoted by * and **, respectively.

neuronal differentiation ability of NSCs, and irradiation caused further inhibition.

When culture in glial differentiation medium, compared with the NSCs cultured alone, the percentage of GFAP-positive cells decreased by 16%, 25% and 43% after co-culture with sham-irradiated, 0.1 and 2 Gy-irradiated bEnd.3 cells, respectively (Fig. 5a and 5b). Moreover, the total number of protrusions and the mean length of the longest protrusion of 50 GFAP-positive cells in each group were examined. The results show that the glial cells differentiated from the NSCs cultured alone had (94 ± 7) protrusions with an average length of

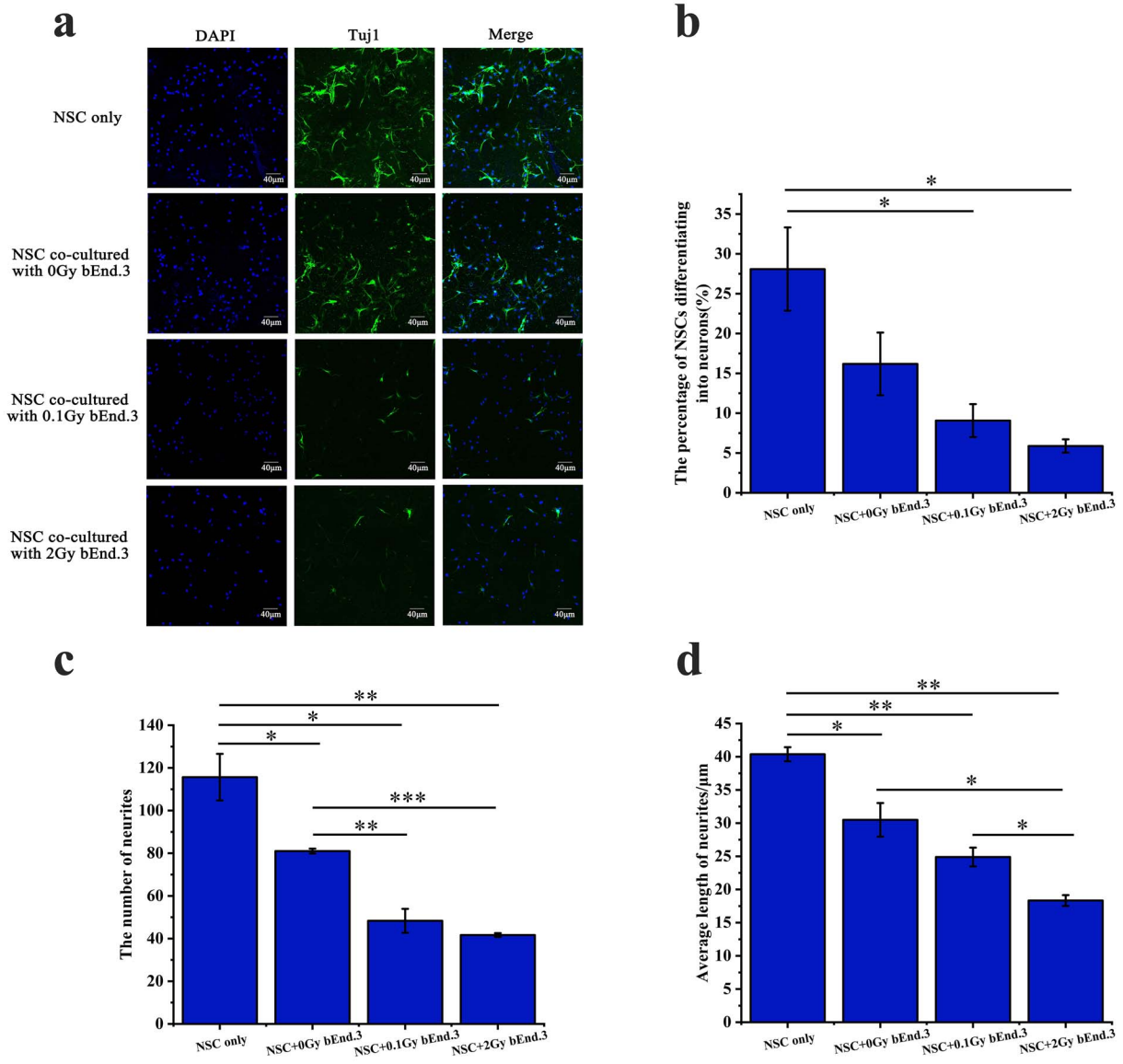

Fig. 4. The differentiation ability of NSCs was inhibited after co-culture with bEnd.3 cells. (a) Fluorescence images of neuronal cells differentiated from different groups of NSCs. Blue and green fluorescence indicate DAPI and Tuj1 staining, respectively. (b) Quantitative analysis of Tuj1-positive cell rate of each group. (c) Total number of the neurites of 50 Tuj1-positive cells in each group. (d) Mean length of the longest neurites of 50 Tuj1-positive cells in each group. $p < 0.05$, 0.01 and 0.001 between two groups are denoted by *, ** and ***, respectively.

(40.14 ± 4.06) μm for the longest protrusions, while the glial cells differentiated from the NSCs co-cultured with sham-irradiated bEnd.3 cells had (68 ± 4) protrusion with an average length of (30.75 ± 3.03) μm for the longest protrusions. For the group of NSCs co-cultured with 0.1 Gy irradiated-bEnd.3 cells, the glial cells had (48 ± 6) protrusion with an average length of (27.33 ± 2.41) μm for the longest protrusions. For the group of NSCs co-cultured with 2 Gy irradiated- bEnd.3 cells, the glial cells had (48 ± 7) protrusions with an average length of (22.64 ± 1.01) μm for the longest protrusions (Fig. 5c and 5d). These data suggested that co-culture with bEnd.3 cells also inhibited the glial differentiation ability of NSCs, and irradiation caused further inhibition.

DISCUSSION

RIND recently has attracted a lot of attention, but the underlying mechanisms are still poorly elucidated. Alterations in vascular and glial cell clonogenic populations, neurogenesis inhibition, altered neuronal function and neuroinflammation induced by IR have been believed to play important roles in RIND [22]. And extensive evidence for

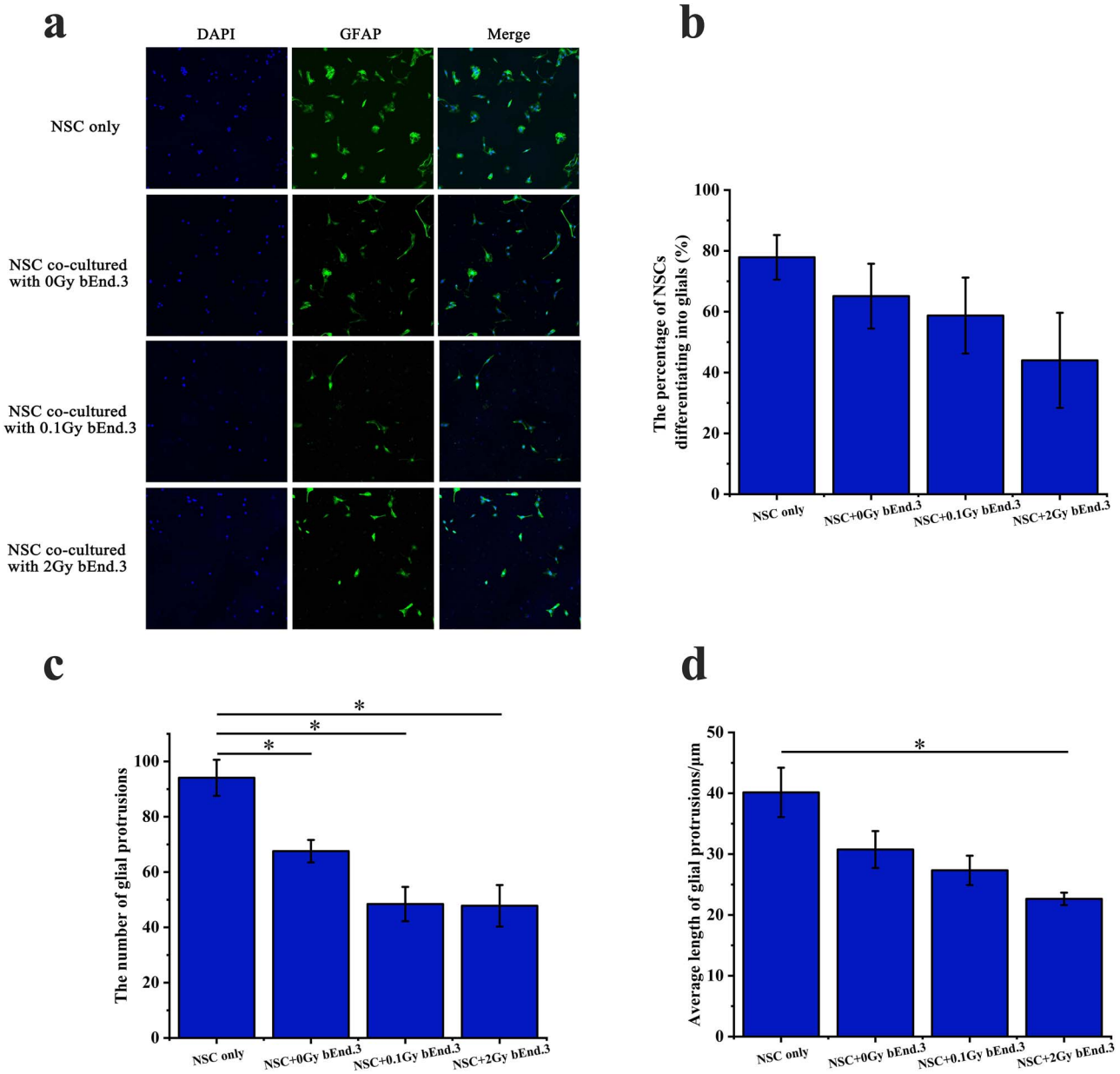

Fig. 5. (a) Fluorescence images of glial cells differentiated from different groups of NSCs. Blue and green fluorescence indicate DAPI and GFAP staining, respectively. (b) Quantitative analysis of GFAP-positive cell rate of each group. (c) Total number of the protrusions of 50 GFAP-positive cells in each group. (d) Mean length of the longest protrusions of 50 GFAP-positive cells in each group. $p < 0.05$ between two groups is denoted by *.

the involvement of these CNS changes in RIND has been provided [15]. Among these changes, radiation-induced alterations in vascular cell population may contribute to the occurrence of RIND via two mechanisms. First, it has long been recognized that vascular disruption can be induced quickly (within hours) by a single dose of radiation, followed by vascular dysfunction several months later [23, 24]. Further studies revealed that irradiation can cause significant endothelial cell loss through apoptosis within a day, which persists for months [25–27]. In this study, we observed significant apoptosis of bEnd.3 endothelial cells 24 h after 4 Gy of X-irradiation (Fig. 1c) and chromosomal damage even at 0.1 Gy, confirming the high radiosensitivity of vascular endothelial cells. Along with glial cell loss, vascular endothelial loss may contribute to white matter damage and subsequent cognitive dysfunction [28]. Secondly, as a vital component of neurogenic niches, microvessels provide a microenvironment suitable for the proliferation, migration and differentiation of NSCs by supplying oxygen, nutrients and soluble factors such as VEGF and fibroblast growth factor-2 [29]. Thus, after exposure, IR-induced decrease in vessel density, increase in vessel permeability and long-lasting hypoxia in the hippocampus [30] may cause neurogenesis inhibition, resulting in cognitive impairment.

In the present study, we provided experimental evidence for the third potential mechanism underlying how the damage in vascular cells may contribute to RIND, i.e. irradiated endothelial cells may induce RIBEs in non-irradiated NSCs, thus inhibiting neurogenesis, in turn leading to RIND. NSCs are actually in physical association with blood vessels in the brain [31]. Therefore, NSCs and endothelial cells may interact with each other through endothelially-secreted factors, contact-dependent signaling, signaling by blood-borne and cerebrospinal fluid (CSF)-borne substances as well as inverted signaling from NSCs to blood vessels [31]. These interactions are similar to RIBE. Thus, it was logic to propose that when radiation cause alterations of these interactions, the proliferation, migration and differentiation of NSCs may be altered. By using a co-culture method, we did find that the medium-mediated interactions between bEnd.3 endothelial cells and NSCs inhibited the cell proliferation, stemness maintenance, neurosphere-forming and differentiation capability of NSCs when compared with the NSCs cultured alone. This is not exactly same as what was previously reported that endothelial cells stimulate NSC expansion and delay differentiation through soluble factors [32]. This discrepancy could be caused by different endothelial cells we used. But more importantly, we found that all the characteristics of NSCs, neuronal differentiation in particular, were further inhibited although no obvious oxidative stress and apoptosis were induced when co-culture with irradiated bEnd.3 cells, indicating that radiation induced bystander effects in non-irradiated NSCs.

RIBE has become a dogma in radiation biology. However, the health consequences of RIBEs remain elucidated and require more investigation. The results from Ivanov *et al.* that irradiated neuroblastoma cells caused apoptosis and suppressed neuronal differentiation of non-irradiated NSCs suggested that irradiated cancer cells may inhibit neurogenesis via RIBEs [9]. Taking a further step by using an *in vivo* system, we clearly demonstrated that RIBEs may contribute to RIND since injection of exosomes from irradiated cancer cells into the hippocampus inhibited neurogenesis and caused cognitive impairment in the recipient mice [11]. Thus, the results we present here suggest that RIBEs of unexposed NSCs induced by irradiated endothelial cells may also contribute to RIND through neurogenesis inhibition.

In summary, here we present the experimental evidence that irradiated endothelial cells induced RIBEs in non-irradiated NSCs manifesting as reduced proliferation, compromised neurosphere-forming capability and impaired differentiation potential, suggesting that damaged vascular cells may contribute to RIND via inducing RIBEs in NSCs resulting in neogenesis inhibition. Further *in vivo* and mechanistic studies are needed to confirm this and explore the detailed mechanisms.

CONFLICT OF INTEREST

The authors declare no conflict of interests.

FUNDING

This study was supported by the National Natural Science Foundation of China (Grant U1632270) and the Priority Academic Program Development of Jiangsu Higher Education Institution (PARD).

REFERENCES

1. Scoccianti S, Detti B, Cipressi S et al. Changes in neurocognitive functioning and quality of life in adult patients with brain tumors treated with radiotherapy. *J Neuro-Oncol* 2012;108:291–308.
2. Gondi V, Tomé WA, Mehta MP. Why avoid the hippocampus? A comprehensive review. *Radiother Oncol* 2010;97:370–6.
3. Redmond KJ, Mahone EM, Terezakis S et al. Association between radiation dose to neuronal progenitor cell niches and temporal lobes and performance on neuropsychological testing in children: a prospective study. *Neuro-Oncology* 2013;15:360–9.
4. Gondi V, Pugh SL, Tome WA et al. Preservation of memory with conformal avoidance of the hippocampal neural stem-cell compartment during whole-brain radiotherapy for brain metastases (RTOG 0933): a phase II multi-institutional trial. *J Clin Oncol* 2014;32:3810–6.
5. Caine C, Deshmukh S, Gondi V et al. CogState computerized memory tests in patients with brain metastases: secondary endpoint results of NRG oncology RTOG 0933. *J Neuro-Oncol* 2016;126:327–36.
6. Oh SB, Park HR, Jang YJ et al. Baicalein attenuates impaired hippocampal neurogenesis and the neurocognitive deficits induced by γ-ray radiation. *Br J Pharmacol* 2013;168:421–31.
7. Zanni G, Goto S, Fragopoulou AF et al. Lithium treatment reverses irradiation-induced changes in rodent neural progenitors and rescues cognition. *Mol Psychiatry* 2021;26:322–40.
8. Acharya MM, Christie LA, Lan ML et al. Human neural stem cell transplantation ameliorates radiation-induced cognitive dysfunction. *Cancer Res* 2011;71:4834–45.
9. Ivanov VN, Hei TK. A role for TRAIL/TRAIL-R2 in radiation-induced apoptosis and radiation-induced bystander response of human neural stem cells. *Apoptosis* 2014;19:399–413.
10. Tan W, Zhang Y, Li M et al. miR-27a-containing exosomes secreted by irradiated skin keratinocytes delayed the migration of unirradiated skin fibroblasts. *Int J Biol Sci* 2019;15:2240–55.
11. Yang X, Ma L, Ye Z et al. Radiation-induced bystander effects may contribute to radiation-induced cognitive impairment. *Int J Radiat Biol* 2021;97:329–40.
12. Kempermann G, Gast D, Gage FH. Neuroplasticity in old age: sustained fivefold induction of hippocampal neurogenesis by long-term environmental enrichment. *Ann Neurol* 2002;52:135–43.
13. Dulken BW, Buckley MT, Navarro Negredo P et al. Single-cell analysis reveals T cell infiltration in old neurogenic niches. *Nature* 2019;571:205–10.
14. Monje ML, Mizumatsu S, Fike JR et al. Irradiation induces neural precursor-cell dysfunction. *Nat Med* 2002;8:955–62.
15. Makale MT, McDonald CR, Hattangadi-Gluth JA et al. Mechanisms of radiotherapy-associated cognitive disability in patients with brain tumours. *Nat Rev Neurol* 2017;13:52–64.
16. Hoorelbeke D, Decrock E, De Smet M et al. Cx43 channels and signaling via IP3/Ca2+, ATP, and ROS/NO propagate radiation-induced DNA damage to non-irradiated brain microvascular endothelial cells. *Cell Death Dis* 2020;11:194.

17. Shi W, Liu W, Ma J et al. The role of Atg7-mediated autophagy in ionizing radiation-induced neural stem cell damage. *Gene* 2020;738:144485.
18. Sasaki R, Aoki S, Yamato M et al. A protocol for immunofluorescence staining of floating neurospheres. *Neurosci Lett* 2010;479:126–7.
19. Azzam EI, de Toledo SM, Little JB. Oxidative metabolism, gap junctions and the ionizing radiation-induced bystander effect. *Oncogene* 2003;22:7050–7.
20. Klammer H, Mladenov E, Li F et al. Bystander effects as manifestation of intercellular communication of DNA damage and of the cellular oxidative status. *Cancer Lett* 2015;356: 58–71.
21. Mignone JL, Kukekov V, Chiang AS et al. Neural stem and progenitor cells in nestin-GFP transgenic mice. *J Comp Neurol* 2004;469:311–24.
22. Greene-Schloesser D, Moore E, Robbins ME. Molecular pathways: radiation- induced cognitive impairment. *Clin Cancer Res* 2013;19:2294–300.
23. Gerstner HB, Brooks PM, Smith SA. Effect of x-radiation on the flow of perfusion fluid through the isolated rabbit's ear. *Am J Phys* 1955;182:459–61.
24. Krueger H, Wagelie EG, Bogart R. Radiation and responses of rabbit ear artery to xylene, alcohol, and epinephrine. *Radiat Res* 1967;30:420–30.
25. Ljubimova NV, Levitman MK, Plotnikova ED et al. Endothelial cell population dynamics in rat brain after local irradiation. *Br J Radiol* 1991;64:934–40.
26. Peña LA, Fuks Z, Kolesnick RN. Radiation-induced apoptosis of endothelial cells in the murine central nervous system: protection by fibroblast growth factor and sphingomyelinase deficiency. *Cancer Res* 2000;60:321–7.
27. Li YQ, Chen P, Haimovitz-Friedman A et al. Endothelial apoptosis initiates acute blood-brain barrier disruption after ionizing radiation. *Cancer Res* 2003;63:5950–6.
28. Calvo W, Hopewell JW, Reinhold HS et al. Time- and dose-related changes in the white matter of the rat brain after single doses of X rays. *Br J Radiol* 1988;61:1043–52.
29. Hatakeyama M, Ninomiya I, Kanazawa M. Angiogenesis and neuronal remodeling after ischemic stroke. *Neural Regen Res* 2020;15:16–9.
30. Warrington JP, Csiszar A, Johnson DA et al. Cerebral microvascular rarefaction induced by whole brain radiation is reversible by systemic hypoxia in mice. *Am J Physiol Heart Circ Physiol* 2011;300:736–44.
31. Licht T, Keshet E. The vascular niche in adult neurogenesis. *Mech Dev* 2015;138:56–62.
32. Shen Q, Goderie SK, Jin L et al. Endothelial cells stimulate self-renewal and expand neurogenesis of neural stem cells. *Science* 2004;304:1338–40.